Nonlinear Dyn (2014) 78:251–263
DOI 10.1007/s11071-014-1437-7

ORIGINAL PAPER

A general mechanism to generate three limit cycles in planar Filippov systems with two zones

Emilio Freire · Enrique Ponce · Francisco Torres

Received: 14 November 2013 / Accepted: 2 May 2014 / Published online: 24 May 2014

Abstract Discontinuous piecewise linear systems with two zones are considered. A general canonical form that includes all the possible configurations in planar linear systems is introduced and exploited. It is shown that the existence of a focus in one zone is sufficient to get three nested limit cycles, independently on the dynamics of the another linear zone. Perturbing a situation with only one hyperbolic limit cycle, two additional limit cycles are obtained by using an adequate parametric sector of the unfolding of a codimension-two focus-fold singularity.

Keywords Discontinuous piecewise linear systems · Liénard equation · Limit cycles

1 Introduction and statement of main results

Planar piecewise linear systems (planar PWL systems, for short) are extensively studied since they are capable to model different devices and process appearing in mechanics, electronics and economy, among other fields, see for instance [1,6,19]. Frequently, such models contain several parameters and it is crucial to determine the response of the system under study for the different values of the parameters, getting so a global understanding of all possible dynamical behaviors. One of the possible final behaviors is the occurrence of self-sustained oscillations, being the number and stability character of these isolated periodic solutions, also called limit cycles, one important issue in the field. Nowadays, as explained below, the specific case of discontinuous PWL systems with two zones is receiving a great attention, because even in these simple cases it is a non-trivial problem to characterize such a number of limit cycles; in fact, this problem can be seen as a particular instance of 16th Hilbert's problem and it is by no means solved at all.

The determination of upper bounds for the number of limit cycles in all possible configurations within the family of planar PWL systems with two zones has been the subject of some recent papers. First, Han and Zhang [12] conjectured in 2010 that general planar PWL systems with two linear zones have at most two limit cycles. In 2012, Huan and Yang [13] gave a negative answer to this conjecture by means of a concrete example with three limit cycles under a rather specific focus-focus configuration. This numerical example greatly stimulated the research to verify this fact and a computer assisted proof was given in [17]. Recently, in [3] one can find a study showing that the three limit cycles

E. Freire · E. Ponce (✉)
Departamento de Matemática Aplicada, Escuela Técnica Superior de Ingeniería, Avda. de los Descubrimientos, 41092 Sevilla, Spain
e-mail:eponcem@us.es

E. Freire
e-mail:efrem@us.es

F. Torres
Departamento de Matemática Aplicada, Escuela Politécnica Superior, Virgen de Africa, 7, 41011 Sevilla, Spain
e-mail:ftorres@us.es

of the Huan and Yang's example can be simultaneously obtained through a boundary equilibrium bifurcation. Later, a general and analytical proof for the existence of three nested limit cycles in certain open regions of the parameter space in the focus-focus configuration has been given in [9]. This number three seems to be the maximum number of limit cycles that can be obtained through piecewise linear perturbation of a linear center, see [5]. When the boundary between linear zones is not a straight line the situation is completely different and it seems possible to obtain as much cycles as you want, see [4]. Regarding other configurations, several examples leading to the existence of at least two limit cycles in the focus-saddle and in the node-saddle cases have appeared in [16]. The general node–node case has been studied in [14] while saddle–saddle cases appeared in [2,15,18].

In this paper, we present for the first time a general canonical form that includes all the possible configurations in planar linear systems, see Proposition 2. This normalized canonical forms helped us to obtain other relevant results. Thus, we improve the lower bounds for the maximum number of limit cycles by showing that it suffices a focus zone to have at least three limit cycles, independently of the dynamics in the other zone. More specifically, we prove that one can have three limit cycles not only in the focus-focus case, as shown in [9], so that the lower bounds for the maximum number of limit cycles corresponding both to the focus-node and focus-saddle cases is 3, one more than stated before, see [16].

The key point for getting the aforementioned three limit cycles is to select parameters in such a way that we have a focus-fold singularity at the origin, see [11], and simultaneously one non-local crossing limit cycle surrounding the origin. As a second and final step, we move the two crucial parameters that unfold the codimension two singularity, by entering in a parametric sector of the unfolding where two new small crossing limit cycles appear, so obtaining a phase plane with three nested limit cycles, all of them surrounding the small segment corresponding to the sliding set. Remarkably enough, such a parametric sector is precisely the one lacking in the analysis of the focus-fold singularity included in [11], and pointed out recently in [10].

To start with, let us assume without loss of generality that the linearity regions in the phase plane are the left and right half-planes

$$S^- = \{(x, y) : x < 0\}, \quad S^+ = \{(x, y) : x > 0\},$$

so that $x = 0$ is the separation line and the systems to be studied become

$$\dot{\mathbf{x}} = \mathbf{X}(\mathbf{x}) = \begin{cases} \mathbf{X}^-(\mathbf{x}), & \text{if } \mathbf{x} \in S^-, \\ \mathbf{X}^+(\mathbf{x}), & \text{if } \mathbf{x} \in S^+, \end{cases} \tag{1}$$

where

$$\mathbf{X}^{\pm}(\mathbf{x}) = A^{\pm}\mathbf{x} + \mathbf{b}^{\pm},$$

and $\mathbf{x} = (x, y)^T \in \mathbb{R}^2$, $A^- = (a_{ij}^-)$, $A^+ = (a_{ij}^+)$ are 2×2 constant matrices, and $\mathbf{b}^- = (b_1^-, b_2^-)^T$, $\mathbf{b}^+ = (b_1^+, b_2^+)^T$ are constant vectors of $\mathbb{R}^2$.

The above discontinuous PWL systems (DPWL systems, for short) have in principle 12 parameters and so their complete analysis seems to be an impossible task. Through some change of variables, we obtain an adequate canonical form with few parameters which is, in all the relevant aspects concerning limit cycles, topologically equivalent to system (1), see [8].

By denoting as T^- and T^+ the traces and as D^- and D^+ the determinants of matrices A^- and A^+, the following result can be stated, see Proposition 3.1 in [8].

Proposition 1 (Liénard canonical form for DPWL systems) *Assume that $a_{12}^+ a_{12}^- > 0$ in system (1). Then the homeomorphism $\tilde{\mathbf{x}} = h(\mathbf{x})$ given by*

$$\tilde{\mathbf{x}} = \begin{pmatrix} 1 & 0 \\ a_{22}^- & -a_{12}^- \end{pmatrix} \mathbf{x} - \begin{pmatrix} 0 \\ b_1^- \end{pmatrix}, \text{ if } \mathbf{x} \in S^-,$$

$$\tilde{\mathbf{x}} = \frac{1}{a_{12}^+} \begin{pmatrix} a_{12}^- & 0 \\ a_{12}^- a_{22}^+ & -a_{12}^- a_{22}^+ \end{pmatrix} \mathbf{x} - \begin{pmatrix} 0 \\ b_1^- \end{pmatrix}, \text{ if } \mathbf{x} \in S^+,$$

after dropping tildes, transforms system (1) into the Liénard canonical form,

$$\begin{aligned} \dot{\mathbf{x}} &= \begin{pmatrix} T^- & -1 \\ D^- & 0 \end{pmatrix} \mathbf{x} - \begin{pmatrix} 0 \\ a^- \end{pmatrix}, \text{ if } \mathbf{x} \in S^-, \\ \dot{\mathbf{x}} &= \begin{pmatrix} T^+ & -1 \\ D^+ & 0 \end{pmatrix} \mathbf{x} - \begin{pmatrix} -b \\ a^+ \end{pmatrix}, \text{ if } \mathbf{x} \in S^+, \end{aligned} \tag{2}$$

where $a^- = a_{12}^- b_2^- - a_{22}^- b_1^-$, and

$$b = \frac{a_{12}^-}{a_{12}^+} b_1^+ - b_1^-, \quad a^+ = \frac{a_{12}^-}{a_{12}^+}(a_{12}^+ b_2^+ - a_{22}^+ b_1^+).$$

There is a topological equivalence between systems (1) and (2) for all the orbits not having points in common with the sliding set, that is, the segment of the y-axis between the tangency points $(0, b)$ and $(0, 0)$.

Besides the invariance of the separation line, the crossing and sliding sets, tangency points, and boundary equilibria of the original system (1) are transformed by the homeomorphism h into sets and points of the same type for system (2). The homeomorphism h also preserves the attractive or repulsive character of the sliding set.

By considering the signs of the discriminants $\Delta^{\pm} = (T^{\pm})^2 - 4D^{\pm}$ of the characteristic equations of 2×2 matrices in (2), we introduce the *modal* parameters $m_{\{R,L\}} \in \{i, 0, 1\}$ defined for each zone by

$$m = \begin{cases} i & \text{if } T^2 - 4D < 0, \\ 0 & \text{if } T^2 - 4D = 0, \\ 1 & \text{if } T^2 - 4D > 0, \end{cases} \tag{3}$$

standing the symbol i for the imaginary unit of the complex plane such that $i^2 = -1$. Also, we normalize the time in a different way for each zone, to rewrite the previous Liénard canonical form in a more convenient form for the subsequent analysis.

Proposition 2 (Normalized canonical form) *The canonical form (2) can be rewritten as*

$$\begin{aligned} \dot{\mathbf{x}} &= \begin{pmatrix} 2\gamma_L & -1 \\ \gamma_L^2 - m_L^2 & 0 \end{pmatrix} \mathbf{x} - \begin{pmatrix} 0 \\ a_L \end{pmatrix} \text{ if } \mathbf{x} \in S^-, \\ \dot{\mathbf{x}} &= \begin{pmatrix} 2\gamma_R & -1 \\ \gamma_R^2 - m_R^2 & 0 \end{pmatrix} \mathbf{x} - \begin{pmatrix} -b \\ a_R \end{pmatrix} \text{ if } \mathbf{x} \in S^+, \end{aligned} \tag{4}$$

where the modal parameters $m_{\{R,L\}} \in \{i, 0, 1\}$ are defined in (3). Accordingly, the new constant terms $a_{\{R,L\}}$ and normalized semi-traces $\gamma_{\{R,L\}}$ are

$$a_{\{R,L\}} = \frac{a^{\pm}}{\omega_{\{R,L\}}}, \quad \gamma_{\{R,L\}} = \frac{T^{\pm}}{2\omega_{\{R,L\}}}, \tag{5}$$

being $\omega_{\{R,L\}} = 1$ for $m_{\{R,L\}} = 0$, while

$$\omega_{\{R,L\}} = \sqrt{\left| \frac{(T^{\pm})^2}{4} - D^{\pm} \right|} \text{ if } m_{\{R,L\}} \neq 0.$$

Proof First consider the left zone. If we do in (2) for $x < 0$ the change of variables

$$(x, y, t) \to \left(\frac{x}{\omega_L}, y, \frac{t}{\omega_L} \right),$$

then the left system turns out to be

$$\dot{\mathbf{x}} = \begin{pmatrix} \frac{T^-}{\omega_L} & -1 \\ \frac{D^-}{\omega_L^2} & 0 \end{pmatrix} \mathbf{x} - \begin{pmatrix} 0 \\ \frac{a^-}{\omega_L} \end{pmatrix}.$$

Taking into account (5) and the relationship $4m_L^2\omega_L^2 = (T^-)^2 - 4D^-$, which is always true, we obtain

$$\gamma_L^2 - m_L^2 = \frac{(T^-)^2}{4\omega_L^2} - m_L^2 = \frac{D^-}{\omega_L^2},$$

and the canonical form for the left system given in (4) follows.

The proof for the right zone is similar and will not be shown. □

It should be noticed the meaning of the modal parameters regarding the type of dynamics in each zone. Thus, for $m = i$ we have a focus; for $m = 0$ we have a improper node; when $m = 1$ we have a node if $|\gamma| \geq 1$ and a saddle if $|\gamma| < 1$. We see that the condition $\gamma^2 - m^2 < 0$ leads to saddle cases, while $\gamma^2 - m^2 \geqslant 0$ corresponds to anti-saddle cases. We also note that $\gamma^2 - m^2 = 0$ only occurs for the node cases $|\gamma| = m = 1$ and $\gamma = m = 0$ which, excepting the degenerate case $a = 0$, correspond to a system with no finite equilibrium points.

The usefulness of the normalized canonical form will be patent at once. We start from system (4) and look for crossing periodic orbits with only one equilibrium in its interior. We study the case having a real unstable focus in the left zone ($m_L = i, \gamma_L > 0, a_L \leqslant 0$), see Fig. 1. We will see that it is not difficult to find situations with one, two, or three crossing periodic orbits whatever be the kind of dynamics in the right zone.

Obviously, to have a crossing periodic orbit, we need for some points of the discontinuity line $x = 0$ to be transformed by means of the flow of the right zone into points of the same line. To obtain such a return of the

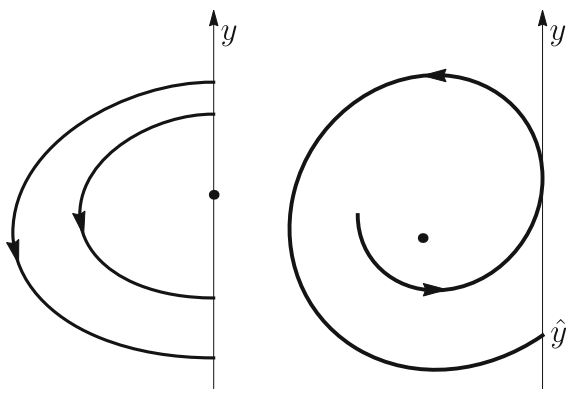

Fig. 1 Two different configurations for the *left zone*. *Left panel* boundary focus. *Right panel* a real focus with the orbit leading to the visible tangency at the origin

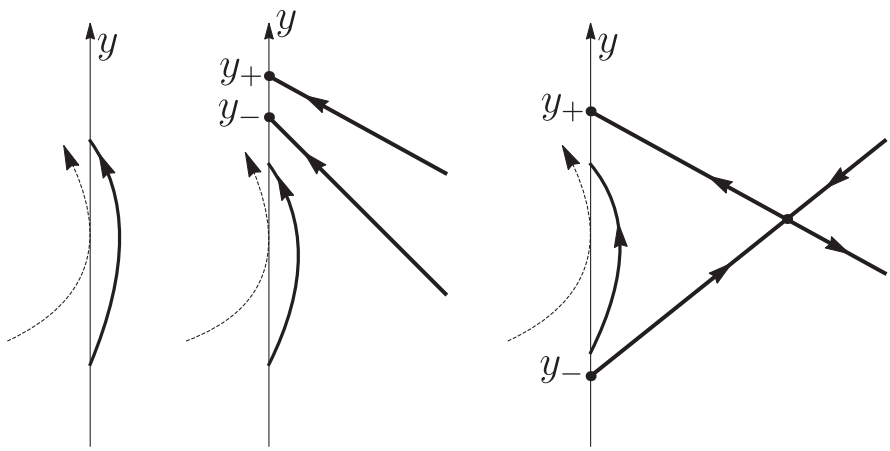

Fig. 2 Three different configurations for the *right zone* when the orbits return to the *left zone*. *Dashed lines* denote the invisible tangent trajectory. *Left panel* virtual focus. *Central panel* virtual node. *Right panel* real saddle

flow in the right zone it suffices to consider either an anti-saddle dynamics (induced by a virtual focus or by a virtual node, not to have more equilibrium points inside the periodic orbit) or a saddle dynamics (induced then by a real saddle to be located outside the periodic orbit), see Fig 2. From Proposition 3.7 in [8], we can anticipate that when there is no sliding motion, that is $b = 0$, the dynamics in the right zone must be contractive ($\gamma_R < 0$). The above considerations suggest to consider the family of systems

$$\begin{aligned} \dot{\mathbf{x}} &= \begin{pmatrix} 2\gamma_L & -1 \\ \gamma_L^2 + 1 & 0 \end{pmatrix} \mathbf{x} - \begin{pmatrix} 0 \\ a_L \end{pmatrix} \text{ if } \mathbf{x} \in S^-, \\ \dot{\mathbf{x}} &= \begin{pmatrix} 2\gamma_R & -1 \\ \gamma_R^2 - m_R^2 & 0 \end{pmatrix} \mathbf{x} - \begin{pmatrix} -b \\ a_R \end{pmatrix} \text{ if } \mathbf{x} \in S^+, \end{aligned} \tag{6}$$

with $m_R \in \{i, 0, 1\}$, under the restrictions

$$\gamma_L > 0, \quad a_L \leqslant 0, \quad \gamma_R < 0, \quad a_R < 0.$$

Our first main result is of global character and concerns the case of the left focus at the boundary ($a_L = 0$, called *boundary focus*) and no proper sliding set ($b = 0$) but with an invisible tangency or *fold* on the right zone, a situation leading to the so called *focus-fold* singularity, see [11]. For our discontinuous piecewise linear systems (6), such a singularity is compatible with the existence of one non-local crossing periodic orbit for all possible dynamics in the right zone.

Proposition 3 *Assume $a_L = 0$ (boundary focus) and $b = 0$, $a_R < 0$ (invisible tangency at the origin), $\gamma_R < 0$ in system (6). Take $m_R \in \{i, 0, 1\}$. Then there exists $\gamma_L > 0$ such that system (6) has one hyperbolic stable crossing periodic orbit surrounding the origin.*

Our second main result has a local flavor and assures the existence of at least two crossing periodic orbits in system (6) for a certain parameter region near the origin of plane (a_L, b). These two crossing periodic orbits bifurcate from the origin of the phase plane in passing from the parameter situation $a_L = b = 0$ to a certain perturbed situation with the focus already in the left region ($a_L < 0$) and with a small repelling sliding set ($b < 0$).

Proposition 4 *Assume $\gamma_L > 0, a_R < 0, \gamma_R < 0$, and take $m_R \in \{i, 0, 1\}$ in system (6). Then there exist $\xi > 0$ and two continuous functions η_1, η_2, satisfying $\eta_1(0) = \eta_2(0) = 0$ and $\eta_1(\varepsilon) < \eta_2(\varepsilon) < 0$ for $-\xi < \varepsilon < 0$, such that for the parameter sector defined by $-\xi < a_L < 0$ and $\eta_1(a_L) < b < \eta_2(a_L)$ system (6) has at least two nested crossing periodic orbits.*

Both periodic orbits surround the sliding segment $\{(0, y) : b \leqslant y \leqslant 0\}$ and they have opposite stabilities, the bigger one being unstable and including in its interior the stable one. When $(a_L, b) \to (0, 0)$ within the above sector, both periodic orbits decrease in size, eventually shrinking to the origin.

Both Propositions 3 and 4 are proved in Sect. 3, after a thorough study of Poincaré half-return maps, see Sect. 2. Our final result, which is a logical consequence of these two previous ones, assures the existence of at least three nested crossing periodic orbits in system (6) when we select adequately the parameter values of the family.

Theorem 1 *Assume $a_R < 0, \gamma_R < 0$, and $m_R \in \{i, 0, 1\}$ in system (6). Then there exist $\gamma_L > 0, \xi > 0$ and two continuous functions η_1, η_2, with $\eta_1(0) = \eta_2(0) = 0$ and satisfying $\eta_1(\varepsilon) < \eta_2(\varepsilon) < 0$ for $-\xi < \varepsilon < 0$, such that for $-\xi < a_L < 0$ and*

$\eta_1(a_L) < b < \eta_2(a_L)$ system (6) has at least three nested crossing periodic orbits.

Proof From Proposition 3, for $a_L = b = 0$ there exists $\gamma_L > 0$ such that system (6) has one hyperbolic stable crossing periodic orbit. Once selected such a value of $\gamma_L > 0$, and according to Proposition 4, by perturbing the parameters a_L and b under the conditions $-\xi < a_L < 0$ and $\eta_1(a_L) < b < \eta_2(a_L)$ system (6) has two new crossing periodic orbits with opposite stabilities, the bigger being unstable. Since the first periodic orbit is stable and persists due to its hyperbolicity, the perturbed system has at least three crossing periodic orbits. □

The rest of the paper is organized as follows. Next, we give the main properties of Poincaré maps, needed to show the above results. Finally, in Sect. 3, the proofs of intermediate results used to show Theorem 1 are included.

2 Poincaré maps

We start this section by giving the expressions of the matrix exponential e^{At}, to be needed at once, where matrix A has the form indicated in (4), that is

$$A = \begin{pmatrix} 2\gamma & -1 \\ \gamma^2 - m^2 & 0 \end{pmatrix}$$

with $m \in \{i, 0, 1\}$. First, let us introduce the functions

$$C_m(t) = \cosh(mt), \quad S_m(t) = \begin{cases} \frac{\sinh(mt)}{m}, & \text{if } m \neq 0, \\ t, & \text{if } m = 0. \end{cases}$$

Note that $C_0(t) \equiv 1$ and that for $m = i$ we have

$$C_i(t) = \cosh(it) = \cos t, \quad S_i(t) = \frac{\sinh(it)}{i} = \sin t,$$

and they satisfy $C_m(-t) = C_m(t)$, $S_m(-t) = -S_m(t)$, $C_m^2 - m^2 S_m(t) = 1$,

with derivatives

$$C_m'(t) = m^2 S_m(t), \; S_m'(t) = C_m(t),$$

among some other properties. Then, we have

$$e^{At} = e^{\gamma t} \begin{pmatrix} C_m(t) + \gamma S_m(t) & -S_m(t) \\ (\gamma^2 - m^2) S_m(t) & C_m(t) - \gamma S_m(t) \end{pmatrix}. \quad (7)$$

Let us consider the system

$$\dot{\mathbf{x}} = \begin{pmatrix} 2\gamma & -1 \\ \gamma^2 - m^2 & 0 \end{pmatrix} \mathbf{x} - a\mathbf{e}_2, \quad (8)$$

where from now on we denote with $\mathbf{e}_1 = (1, 0)^T$ and $\mathbf{e}_2 = (0, 1)^T$ the canonical vectors.

Assume the existence of one unstable real focus and consider the orbits evolving on the left half-plane starting at points $(0, y)$ of the y-axis and eventually coming back to the quoted axis at a point $(0, y_1)$. Due to the sense of the flow on the line $x = 0$, we must have $y \geq 0$, $y_1 \leq 0$. Also, there exists one value $\hat{y} \leqslant 0$ such that the solution passing through the origin in a visible (from the left) tangency point to the y-axis terminates at the point $(0, \hat{y})$, with $\hat{y} < 0$, see Fig. 1. In the limiting case of a boundary focus the tangency is invisible from the left, and we will take $\hat{y} = 0$. In any case, the points $y\mathbf{e}_2$ with $y > 0$ are transformed in points $y_1\mathbf{e}_2$ with $y_1 < \hat{y}$. Then, we define the left Poincaré map P_L as $y_1 = P_L(y)$, also taking $P_L(0) = \hat{y}$.

Next, we will parameterize the map P_L. As the system is linear, to compute the Poincaré map is equivalent to find the smaller positive value of t such that

$$\begin{aligned} y_1\mathbf{e}_2 &= e^{At}\left(y\mathbf{e}_2 - a\int_0^t e^{-As}\mathbf{e}_2 ds\right) \\ &= ye^{At}\mathbf{e}_2 - aV(t)\mathbf{e}_2, \end{aligned} \quad (9)$$

where the matrix function $V(t)$ is the primitive of the matrix exponential that vanishes for $t = 0$, defined as

$$\begin{aligned} V(t) &= e^{At}\int_0^t e^{-As} ds = \int_0^t e^{A(t-s)} ds \\ &= \int_0^t e^{Au} du. \end{aligned} \quad (10)$$

In the next result, some useful properties of the matrix function V are shown.

Lemma 1 *The matrix function V defined in (10) satisfies $V(-t) = -e^{-At}V(t)$ and its first derivatives are $V^{(k)}(t) = e^{At}A^{k-1}$ for $k \geq 1$. Consequently, the scalar function*

$$f(t) = \mathbf{e}_1^T V(t)\mathbf{e}_2 \quad (11)$$

satisfies $f(0) = 0$ and its first derivatives are

$$f^{(k)}(t) = \mathbf{e}_1^T e^{At} A^{k-1}\mathbf{e}_2, \; k \geqslant 1,$$

which for $t = 0$ reduce to

$$f'(0) = 0, \; f''(0) = -1, \; f^{(k)}(0) = \mathbf{e}_1^T A^{k-1}\mathbf{e}_2, \; k \geqslant 3.$$

Proof From (10) we have

$$V(-t) = \int_0^{-t} e^{Au}du = -\int_0^{t} e^{-Au}du = -e^{-At}V(t).$$

From (10) we know that the first derivative of the function V is $V'(t) = e^{At}$. The successive derivatives directly follow, so that $V^{(k)}(0) = A^{k-1}$ and the assertions about the function f are immediate. □

For the sake of convenience, we resort to the auxiliary function

$$\Psi_{\gamma,m}(t) = 1 - e^{\gamma t}\left[C_m(t) - \gamma S_m(t)\right], \tag{12}$$

whose derivative with respect to t is

$$\Psi'_{\gamma,m}(t) = (\gamma^2 - m^2)S_m(t)e^{\gamma t}. \tag{13}$$

The function $\Psi_{\gamma,m}$ reduces to

$$\Psi_{\gamma,m}(t) = \begin{cases} 1 - e^{\gamma t}\left(\cos t - \gamma \sin t\right), & \text{if } m = i, \\ 1 - e^{\gamma t}\left(1 - \gamma t\right), & \text{if } m = 0, \\ 1 - e^{\gamma t}\left(\cosh t - \gamma \sinh t\right), & \text{if } m = 1. \end{cases}$$

Note also the symmetry properties

$$\Psi_{\gamma,m}(-t) = \Psi_{-\gamma,m}(t), \quad \Psi'_{\gamma,m}(-t) = -\Psi'_{-\gamma,m}(t).$$

Although we only need the real unstable focus case in the left part of system (6), we study next a more general situation for system (8), considering also saddle and node cases. Thus, we must note first that, for the non-focal cases, the left Poincaré map needs not to be defined in the whole semi-axis $y \geqslant 0$. For instance, if $\gamma^2 - m^2 < 0$ then we are in a saddle case (in fact, $m = 1$ but we keep it not substituted to be more general in what follows), and such a saddle point is located at

$$\begin{pmatrix} x_e \\ y_e \end{pmatrix} = \frac{a}{\gamma^2 - m^2}\begin{pmatrix} 1 \\ 2\gamma \end{pmatrix}.$$

Thus, there will be orbits returning to the y-axis on the left half-plane only if $a > 0$, that is, if the saddle is located within such half-plane. Furthermore, the eigenvectors $\mathbf{v}_\pm$ associated to the two eigenvalues $\lambda_\pm = \gamma \pm m$ must satisfy the equation

$$\begin{pmatrix} \gamma \mp m & -1 \\ \gamma^2 - m^2 & -\gamma \mp m \end{pmatrix}\mathbf{v}_\pm = 0,$$

so that we can choose

$$\mathbf{v}_\pm = \begin{pmatrix} 1 \\ \gamma \mp m \end{pmatrix}.$$

The existence of the return map is determined by the intersections with the y-axis of the linear invariant manifolds of the saddle, to be denoted as $y_\pm$, which can be computed by solving for μ in the equation

$$\frac{a}{\gamma^2 - m^2}\begin{pmatrix} 1 \\ 2\gamma \end{pmatrix} + \mu\begin{pmatrix} 1 \\ \gamma \mp m \end{pmatrix} = \begin{pmatrix} 0 \\ y_\pm \end{pmatrix}.$$

We obtain that

$$y_\pm = \frac{2a\gamma}{\gamma^2 - m^2} - \frac{a(\gamma \mp m)}{\gamma^2 - m^2} = a\frac{\gamma \pm m}{\gamma^2 - m^2} = \frac{a}{\gamma \mp m}. \tag{14}$$

In short, the domain of P_L is restricted to $0 < y < y_- = a/(\gamma + m)$ and we have $y_+ = a/(\gamma - m) < P_L(y) < 0$.

For the node cases with $\gamma^2 - m^2 > 0$ we can take advantage of the previous computations, and we also require that $a > 0$, that is, the node needs to be located at the right half-plane so that orbits starting at the y-axis can return to the same axis in the left half-plane. Now the two intersection ordinates $y_\pm$ have the same sign. For unstable nodes, we have $\gamma > 0$ and $0 < y_- < y_+$ and the domain of P_L is also restricted to $0 < y < y_- = a/(\gamma + m)$ with $P_L(y)$ taking all negative values. For stable nodes, we have $\gamma < 0$ and now $y_- < y_+ < 0$, being P_L defined for all $y > 0$ with $y_+ = a/(\gamma - m) < P_L(y) < 0$.

With these considerations in mind, we state a general result for the left Poincaré map, including all the possible configurations. For sake of brevity, we do not give the range of admissible values for t in each case, as it is not needed for the subsequent analysis.

Proposition 5 *Consider the restriction of system (8) to the region $x \leqslant 0$. The following statements hold.*

(a) If $a = 0$, the left Poincaré map only exists when the dynamics of the system is of focus type and then we have $P_L(y) = -e^{\gamma\pi}y$ for all $y \geqslant 0$.

(b) If both $a \neq 0$ and $\gamma^2 - m^2 \neq 0$, and we additionally assume $a > 0$ for the non-focal cases ($m \neq i$), then the left Poincaré map is given in its domain by

$$y = a\frac{\Psi_{\gamma,m}(t)}{\Psi'_{\gamma,m}(t)} = a\frac{1 - e^{\gamma t}\left[C_m(t) - \gamma S_m(t)\right]}{(\gamma^2 - m^2)S_m(t)e^{\gamma t}},$$
$$P_L(y) = a\frac{\Psi_{\gamma,m}(-t)}{\Psi'_{\gamma,m}(-t)} = -a\frac{1 - e^{-\gamma t}\left[C_m(t) + \gamma S_m(t)\right]}{(\gamma^2 - m^2)S_m(t)e^{-\gamma t}}, \tag{15}$$

(c) *If* $|\gamma| = m = 1$ *and* $a > 0$ *then the left Poincaré map is given by*

$$y = a\frac{e^{2\gamma t} - 1 - 2\gamma t}{2\gamma(e^{2\gamma t} - 1)}, \quad P_L(y) = a\frac{e^{-2\gamma t} - 1 + 2\gamma t}{2\gamma(e^{-2\gamma t} - 1)}, \tag{16}$$

(d) *If* $\gamma = 0$ *and we additionally assume* $a > 0$ *for the non-focal cases* ($m \neq i$)*, then we have* $P_L(y) = -y$ *in its domain.*

(e) *The first derivative of the Poincaré map is given by*

$$P_L'(y) = \frac{y}{P_L(y)}e^{2\gamma t} < 0, \tag{17}$$

and when $a\gamma \neq 0$*, the second derivative satisfies* $\gamma P_L''(y) < 0$.

Proof We start by resorting to Lemma 1. Multiplying (9) from the left by $\mathbf{e}_1^T$ and $\mathbf{e}_1^T e^{-At}$, respectively, we get

$$y_1 \mathbf{e}_1^T \mathbf{e}_2 = 0 = y\mathbf{e}_1^T e^{At}\mathbf{e}_2 - a\mathbf{e}_1^T V(t)\mathbf{e}_2, \tag{18}$$

and

$$y_1 \mathbf{e}_1^T e^{-At}\mathbf{e}_2 = y\mathbf{e}_1^T e^{-At}e^{At}\mathbf{e}_2 - a\mathbf{e}_1^T e^{-At}V(t)\mathbf{e}_2,$$

so that, using again $\mathbf{e}_1^T\mathbf{e}_2 = 0$, we obtain

$$y_1 \mathbf{e}_1^T e^{-At}\mathbf{e}_2 = -a\mathbf{e}_1^T V(-t)\mathbf{e}_2. \tag{19}$$

When $a = 0$ is very easy to see that the Poincaré map only exists when the equilibrium is a focus. Otherwise, the linear invariant manifolds associated to the origin preclude the existence of the return map. Taking $m = i$, from (7) and (18) we deduce

$$\mathbf{e}_1^T e^{At}\mathbf{e}_2 = -e^{\gamma t}S_i(t) = -e^{\gamma t}\sin t = 0,$$

and so $t = \pi$. Then from (9) we achieve

$$y_1 = P_L(y) = -e^{\gamma\pi}y.$$

When $a \neq 0$ the origin is a visible (invisible) left tangency point for $a < 0$ ($a > 0$). As commented before, we need $a > 0$ for the node cases to guarantee the existence of the half-return map. Then, from (18) and (19), by using the unknown flight time t, we obtain a parametrization of y and $P_L(y)$ as follows,

$$y = a\frac{\mathbf{e}_1^T V(t)\mathbf{e}_2}{\mathbf{e}_1^T e^{At}\mathbf{e}_2}, \quad P_L(y) = -a\frac{\mathbf{e}_1^T V(-t)\mathbf{e}_2}{\mathbf{e}_1^T e^{-At}\mathbf{e}_2}, \tag{20}$$

as long as $\mathbf{e}_1^T e^{At}\mathbf{e}_2 = -e^{\gamma t}S_m(t) \neq 0$. Taking into account Lemma 1 and by using the function f defined in (11), we write expressions (20) as

$$y = a\frac{f(t)}{f'(t)}, \quad P_L(y) = a\frac{f(-t)}{f'(-t)}. \tag{21}$$

From (10) and (13), we obtain

$$f(t) = \mathbf{e}_1^T V(t)\mathbf{e}_2 = -\int_0^t S_m(u)e^{\gamma u}du,$$

and thus,

$$f(t) = \begin{cases} -\dfrac{\Psi_{\gamma,m}(t)}{\gamma^2 - m^2}, & \text{if } \gamma^2 \neq m^2, \\ -\dfrac{e^{2\gamma t} - 1 - 2\gamma t}{4}, & \text{if } |\gamma| = m = 1, \\ -\dfrac{t^2}{2}, & \text{if } \gamma = m = 0, \end{cases}$$

and $f'(t) = \mathbf{e}_1^T e^{At}\mathbf{e}_2 = -e^{\gamma t}S_m(t)$, so that expressions (15) and (16) follow. Statements (b) and (c) are shown.

When $\gamma = 0$ and $m \neq 0$ it is easy to see from statements (a) and (b) that $P(y) = -y$. The case $m = 0$ comes from (21) and the corresponding values for $f(t)$ and $f'(t)$. Statement (d) follows.

To show statement (e) when $a \neq 0$ and $\gamma^2 - m^2 \neq 0$, we see from (15) through direct computations that

$$\frac{dy}{dt} = a\frac{1 - e^{-\gamma t}\left[C_m(t) + \gamma S_m(t)\right]}{(\gamma^2 - m^2)S_m^2(t)} = -\frac{P_L(y)}{S_m(t)}e^{-\gamma t},$$

and

$$\frac{dP_L(y)}{dt} = -a\frac{1 - e^{\gamma t}\left[C_m(t) - \gamma S_m(t)\right]}{(\gamma^2 - m^2)S_m^2(t)} = -\frac{y}{S_m(t)}e^{\gamma t},$$

so that (17), the first derivative of map P_L follows.

The case $a = 0$ comes from statement (a) and the cases with $\gamma^2 - m^2 = 0$ easily come from direct computations.

The second derivative turns out to be

$$P_L''(y) = \begin{cases} 2a^2\dfrac{\sinh(\gamma t) - \gamma S_m(t)}{(\gamma^2 - m^2)P_L^3(y)}e^{3\gamma t}, & \text{if } \gamma^2 \neq m^2, \\ a^2\gamma\dfrac{t\cosh(t) - \sinh(t)}{P_L^3(y)}e^{3\gamma t}, & \text{if } |\gamma| = m = 1, \end{cases} \tag{22}$$

and for $a\gamma \neq 0$ it is direct to show that $\gamma P_L''(y) < 0$. The proof is completed. □

A dual result can be stated for the right half-return map that will not be written for sake of brevity, since one has only to reverse the inequalities concerning the sign of a.

Next we give more specific properties for the Poincaré maps of system (6) in the case of having a left dynamics governed by one real or boundary unstable focus in the left zone, that is $\gamma_L > 0$, $a_L \leq 0$, and one

invisible tangency point in the right zone, that is $a_R < 0$ with $m_R \in \{i, 0, 1\}$. For the sake of convenience, we consider a particular instance of function $\Psi_{\gamma,m}$ defined in (12) when $m = i$, namely,

$$\varphi_\gamma(t) = \Psi_{\gamma,i}(t) = 1 - e^{\gamma t}(\cos t - \gamma \sin t),$$

first introduced in [1], see also [7]. We recall for the function φ_γ the symmetry properties

$$\varphi_\gamma(-t) = \varphi_{-\gamma}(t),\ \varphi_{-\gamma}(-t) = \varphi_\gamma(t),\ \varphi'_\gamma(-t) = -\varphi'_\gamma(t),$$

and the existence for $\gamma > 0$ of a value $\hat{t}$ with $\pi < \hat{t} < 2\pi$ such that $\varphi_\gamma(\hat{t}) = 0$. We start by analyzing the left half-return map.

Proposition 6 (The left Poincaré map in the unstable focus case) *For system (6) the following statements hold.*

(a) When $a_L = 0$ the left Poincaré map is defined for $y \geqslant 0$ as

$$P_L(y) = -e^{\gamma_L \pi} y.$$

(b) Assuming $a_L < 0$ and $\gamma_L > 0$, the left Poincaré map P_L is well defined for $y \geqslant 0$ and is given by the expressions

$$y = a_L \frac{\varphi_{\gamma_L}(t)}{\varphi'_{\gamma_L}(t)} = a_L \frac{1 - e^{\gamma_L t}(\cos t - \gamma_L \sin t)}{(\gamma_L^2 + 1)e^{\gamma_L t} \sin t},$$

$$P_L(y) = a_L \frac{\varphi_{\gamma_L}(-t)}{\varphi'_{\gamma_L}(-t)} = -a_L \frac{1 - e^{-\gamma_L t}(\cos t + \gamma_L \sin t)}{(\gamma_L^2 + 1)e^{-\gamma_L t} \sin t},$$

where $\pi < t \leqslant \hat{t}$, being $\hat{t}$ the only value in $(\pi, 2\pi)$ such that $\varphi_{\gamma_L}(\hat{t}) = 0$.
In particular, we have $P_L(0) = a_L \alpha_0$, where

$$\alpha_0 = \frac{\cos \hat{t} + \gamma_L \sin \hat{t} - e^{\gamma_L \hat{t}}}{(\gamma_L^2 + 1) \sin \hat{t}} = -e^{\gamma_L \hat{t}} \sin \hat{t} > 0.$$

Furthermore, the first two derivatives of map P_L satisfy

$$P'_L(0) = 0,\ P''_L(0) = \frac{e^{2\gamma_L \hat{t}}}{a_L \alpha_0},\ \text{and}\ \lim_{y \to \infty} P'_L(y) = -e^{\gamma_L \pi}. \tag{23}$$

Proof Statement (a) and all the expressions given for P_L in statement (b) directly follow from Proposition 5. The great simplification for α_0 arises after multiplying both terms of the fraction by

$$\cos \hat{t} - \gamma_L \sin \hat{t} = e^{-\gamma_L \hat{t}}.$$

It remains to show the properties concerning the derivatives of the map.

From (17) we obtain $P'_L(0) = 0$. Writing (17) as $P_L(y) P'_L(y) = y e^{2\gamma_L t}$, we get

$$P'_L(y) P'_L(y) + P_L(y) P''_L(y) = e^{2\gamma_L t} + 2\gamma_L y e^{2\gamma_L t} \frac{dt}{dy},$$

and taking $y = 0$ we achieve the expression of $P''_L(0)$ given in (23). Finally, from (17) we obtain

$$\lim_{y \to \infty} P'_L(y) = \lim_{t \to \pi} \frac{\varphi_{\gamma_L}(t)}{\varphi_{\gamma_L}(-t)} = -e^{\gamma_L \pi}.$$

The proposition is shown. □

Remark 1 A key observation concerning the return map associated to the focus is its abrupt qualitative change when the parameter a_L passes through zero. Effectively, from statements (a) and (b) above, the derivative at the origin $P'_L(0)$ passes from the value $-e^{\gamma_L \pi}$ when $a_L = 0$ to suddenly vanish for any value $a_L < 0$. Moreover, from (15)–(17) in Proposition 5, we have $P'_L(0) = -1$ for all $a_L > 0$. Such discontinuity in the derivative is associated to the passing from an invisible tangency to a visible one, so that the flight time passes from $t = 0$ for $a_L > 0$ to the value $t = \hat{t}$ for $a_L < 0$, being $t = \pi$ when $a_L = 0$. This jump encompassing such a boundary equilibrium bifurcation is crucial for the result given in Proposition 4.

Regarding the flow in the right part for $a_R < 0$, integrating the system in the zone S^+ from the point $(0, z)$ with $z \leqslant b$, after a time t we arrive at the point $(0, z_1)$, with $z_1 \geqslant b$. So we can define the right Poincaré map $z_1 = P_R(z)$ with $P_R(b) = b$. Since $a_R < 0$, the point $(0, b)$ is an invisible tangency point and we will not have a boundary equilibrium for the right system. We can repeat the procedure done before for the left Poincaré map, step by step, taking into account that the tangency is not at the origin. Then, to compute the parametric representation of the right Poincaré map, from (21) and subsequent definitions, we just write

$$z - b = \frac{a_R}{S_{m_R}(t) e^{\gamma_R t}} \int_0^t S_{m_R}(u) e^{\gamma_R u} du,$$

$$P_R(z) - b = \frac{a_R}{S_{m_R}(-t) e^{-\gamma_R t}} \int_0^{-t} S_{m_R}(u) e^{\gamma_R u} du. \tag{24}$$

With these expressions, it is now immediate to obtain the properties of the right Poincaré map under the assumptions $a_R < 0$ (invisible tangency) and $\gamma_R < 0$ (opposite divergence with respect to the left zone). We

remark that in the non-focal cases ($m_R \neq i$), recall (14), the linear invariant manifolds intersect the y-axis at the points $(0, z_-)$ and $(0, z_+)$, where

$$z_- = b + \frac{a_R}{\gamma_R + m_R}, \quad z_+ = b + \frac{a_R}{\gamma_R - m_R}, \tag{25}$$

excepting the saddle-node-at-infinity case $m_R = -\gamma_R = 1$, where z_- does not exist. We give first a result concerning its global properties, and next a useful result on local properties around the point $(0, b)$.

Proposition 7 (Global properties of the right half-return map) *For $a_R < 0$ and $\gamma_R < 0$ in system (6) the map P_R satisfies the following statements.*

(a) If we are in the focus case ($m_R = i$), then the map P_R is defined for all $z \leqslant b$ with $P_R(z) \geqslant b$, and its parametric expressions are

$$z = b + a_R \frac{1 - e^{\gamma_R t}(\cos t - \gamma_R \sin t)}{(\gamma_R^2 + 1)\sin t} e^{-\gamma_R t},$$

$$P_R(z) = b - a_R \frac{1 - e^{-\gamma_R t}(\cos t + \gamma_R \sin t)}{(\gamma_R^2 + 1)\sin t} e^{\gamma_R t},$$

where $t \in (0, \pi)$. Its first derivative satisfies

$$\lim_{z \to -\infty} P_R'(z) = e^{\gamma_R \pi}.$$

(b) If $m_R \in \{0, 1\}$ and $\gamma_R^2 - m_R^2 \neq 0$, then the map P_R is defined for all $z \leqslant b$ in the nodal cases, that is $\gamma_R < -m_R$, and only for $z_- < z \leqslant b$ in the saddle cases ($m_R = 1, -1 < \gamma_R < 0$). The map is always bounded, so that $b \leqslant P_R(z) < z_+$, see Fig. 3. Its parametric expressions are

$$z = b + a_R \frac{e^{-\gamma_R t} - C_{m_R}(t) + \gamma_R S_{m_R}(t)}{(\gamma_R^2 - m_R^2) S_{m_R}(t)},$$

$$P_R(z) = b - a_R \frac{e^{\gamma_R t} - C_{m_R}(t) - \gamma_R S_{m_R}(t)}{(\gamma_R^2 - m_R^2) S_{m_R}(t)},$$

where $t \in (0, \infty)$. The first derivative satisfies

$$\lim_{z \to z_-} P_R'(z) = 0$$

in the saddle cases, and $\lim_{z \to -\infty} P_R'(z) = 0$, otherwise.

(c) If $m_R = -\gamma_R = 1$, then the map P_R is defined for all $z \leqslant b$ and is bounded, so that $b \leqslant P_R(z) < z_+$. Its parametric expressions are

$$z = b - a_R \frac{e^{-2t} - 1 + 2t}{2(e^{-2t} - 1)},$$

$$P_R(z) = b - a_R \frac{e^{2t} - 1 - 2t}{2(e^{2t} - 1)},$$

where $t \in (0, \infty)$. The first derivative satisfies

$$\lim_{z \to -\infty} P_R'(z) = 0.$$

In all the cases, for all z where the map is defined, the second derivative satisfies $P_R''(z) < 0$.

Proof Since statements (a), (b), and (c) are easily deduced from Proposition 5, we only concern about the second derivative properties. From (22) we obtain

$$P_R''(z) = \frac{2a_R^2 e^{3\gamma t}}{(P_R(z) - b)^3} \frac{\sinh(\gamma_R t) - \gamma_R S_{m_R}(t)}{\gamma_R^2 - m_R^2}, \tag{26}$$

and it is easy to see that the first factor is positive while the second factor is negative, so we have $P_R''(z) < 0$. □

Proposition 8 (Local properties of the right Poincaré map) *Assuming $a_R < 0$ and $\gamma_R < 0$ in system (6) there exists $\varepsilon > 0$ such that the right Poincaré map P_R given in (24) is well defined for $z \in (b - \varepsilon, b]$; in particular we have $P_R(b) = b$. Its first four derivatives at the point $y = b$ are*

$$P_R'(b) = -1, \quad P_R''(b) = -\frac{8\gamma_R}{3a_R}, \quad P_R'''(b) = -\frac{32\gamma_R^2}{3a_R^2},$$

$$P_R^{IV}(b) = -32\gamma_R \frac{79\gamma_R^2 + 9m_R^2}{45a_R^3}. \tag{27}$$

Proof To alleviate the notation, we introduce the auxiliary variables $u = z - b$ and $v = P_R(z) - b$. From (20) and Lemma 1 we have

$$\frac{u}{a_R} = \frac{t}{2} + \frac{\gamma_R}{6}t^2 + \frac{\gamma_R^2 - m_R^2}{24}t^3 - \frac{\gamma_R(7m_R^2 - 3\gamma_R^2)}{360}t^4 + O(t^5) \tag{28}$$

and

$$\frac{v}{a_R} = -\frac{t}{2} + \frac{\gamma_R}{6}t^2 - \frac{\gamma_R^2 - m_R^2}{24}t^3 - \frac{\gamma_R(7m_R^2 - 3\gamma_R^2)}{360}t^4 + O(t^5). \tag{29}$$

By inverting series (28) we obtain

$$\frac{t}{2} = \frac{u}{a_R} + \frac{2\gamma_R}{3a_R^2}u^2 + \frac{3m_R^2 + 5\gamma_R^2}{9a_R^3}u^3 + \frac{4\gamma_R(27m_R^2 + 17\gamma_R^2)}{135a_R^4}u^4 + O(u^5),$$

and so, substituting in (29), we get

$$v = -u - \frac{4\gamma_R}{3a_R}u^2 - \frac{16\gamma_R^2}{9a_R^2}u^3 - \frac{4\gamma_R(9m_R^2 + 79\gamma_R^2)}{135a_R^3}u^4 + O(u^5),$$

so that

$$P_R(z) = b - (z-b) - \frac{4\gamma_R}{3a_R}(z-b)^2 - \frac{16\gamma_R^2}{9a_R^2}(z-b)^3 - \\ - \frac{4\gamma_R(9m_R^2 + 79\gamma_R^2)}{135a_R^3}(z-b)^4 + O(z-b)^5,$$

and the first four derivatives of map P_R given in (27) follow. □

3 Proofs of the main results

We start by giving the proof of Proposition 3.

Proof (Proof of Proposition 3) To prove this proposition we consider the full Poincaré map $P = P_R \circ P_L$ and study its fixed points. From Proposition 6 (a) we know that the left Poincaré map is a linear function given by $P_L(y) = -e^{\gamma_L \pi} y$, so that $P_L''(y) = 0$ for all y. Therefore, from the last statement of Proposition 7, we deduce that

$$P''(y) = P_R''(P_L(y))(P_L'(y))^2 < 0,$$

and taking into account that $P(0) = 0$, the map P has at most one nontrivial fixed point, that is there exists at most one crossing limit cycle.

Before studying the different cases, we note that the derivative of the Poincaré map at the origin is

$$P'(0) = P_R'(P_L(0))P_L'(0) = e^{\gamma_L \pi} > 1.$$

If the dynamics in the right zone is of stable focus type, that is $m_R = i$ along with $\gamma_R < 0$, the Poincaré map is defined for $y \in (0, \infty)$ and we have that

$$\lim_{y \to \infty} P'(y) = e^{(\gamma_L + \gamma_R)\pi}.$$

If we select $\gamma_L > 0$ in such a way that $\gamma_L + \gamma_R < 0$, then there exists $y_f > 0$ such that the graph of $P(y)$ has a slope $P'(y) < 1$ for all $y > y_f$. Thus, the graph of $P(y)$ eventually crosses the diagonal, the map has a fixed point and the system has a unique crossing limit cycle.

If the dynamics in the right zone is of stable node type, then we have either $m_R = 1$ along with $\gamma_R \leqslant -1$ or $m_R = 0$. Using Proposition 7(b)–(c), the Poincaré map is defined for $y \in (0, \infty)$ and bounded; furthermore,

$$\lim_{y \to \infty} P'(y) = 0.$$

Reasoning as before, we can now conclude that for every value $\gamma_L > 0$ the system has a unique crossing limit cycle.

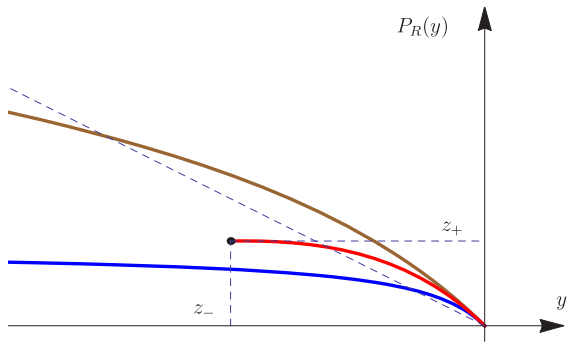

Fig. 3 Typical graphs of the Poincaré map $P_R(y)$ when $b = 0$ and $\gamma_R < 0$ for the node case (in *blue*), the saddle (in *red*) and the focus (in *brown*). Under hypotheses of Proposition 3, the graph of $P_L(y)$ is a *straight line* in the fourth quadrant and, selecting adequately γ_L, the intersection of the graphs of $P_L^{-1}(y)$ (the *dashed oblique line*) and $P_R(y)$ is always possible

If the dynamics in the right zone is of saddle type, that is $m_R = 1$ along with $-1 < \gamma_R < 0$, then the linear invariant manifolds of the saddle intersect the y-axis, recall (25), at

$$z_+ = \frac{a_R}{\gamma_R - 1} > 0, \text{ and } z_- = \frac{a_R}{\gamma_R + 1} < 0,$$

so that the Poincaré map is defined for

$$0 \leqslant y < P_L^{-1}(z_-) = -e^{-\gamma_L \pi} \frac{a_R}{\gamma_R + 1},$$

and its graph is bounded, so that it has its endpoint at $(P_L(z_-), z_+)$. Then, since $P'(0) > 1$ when $\gamma_L > 0$, we have a fixed point and so a crossing periodic orbit, whenever such a final point is under the diagonal, that is

$$\frac{a_R}{\gamma_R - 1} < -e^{-\gamma_L \pi} \frac{a_R}{\gamma_R + 1}$$

or equivalently when

$$0 < \gamma_L < \frac{1}{\pi} \ln \frac{1 - \gamma_R}{1 + \gamma_R}.$$

Since the fixed points of Poincaré map satisfy $P(y) = P_L(P_R(y)) = y$ or equivalently $P_R(y) = P_L^{-1}(y)$, we find in all the cases an explicit range of admissible values of γ_L for which we have a periodic orbit. Furthermore, since it is obvious that at the fixed point $y^* > 0$ where $P(y^*) = y^*$ we have $P'(y^*) < 1$, the periodic orbit is a hyperbolic stable limit cycle and the proposition is shown. A geometrical idea of the proof is given in Fig. 3. □

To finish, we give the proof of Proposition 4.

Proof (Proof of Proposition 4) We start by defining for $y > 0$, in the parameter region with $a_L < 0$ and $b < 0$, the function

$$Q(y) = P_L(y) - P_R^{-1}(y),$$

whose zeros correspond with crossing periodic orbits. Thus, by emphasizing the bifurcation parameters, we study the equation

$$Q(y; a_L, b) = P_L(y; a_L) - P_R^{-1}(y; b) = 0, \qquad (30)$$

for which only solutions with $y > 0$ are meaningful.

From Proposition 8, the derivatives of the right Poincaré map P_R satisfies the following relations,

$$P_R(b) = b, \ P_R'(b) = -1, \ P_R''(b) = -\frac{8\gamma_R}{3a_R} = -2\beta_2,$$

where we have defined the constant $\beta_2 > 0$, and using the involutive character of P_R, see [11], we have

$$P_R^{-1}(y; b) = b - (y - b) - \beta_2(y - b)^2 + O(y - b)^3.$$

To study the solutions of (30), we make the blow-up

$$a_L = -\varepsilon, \quad y = \varepsilon Y, \quad b = \varepsilon B.$$

Note that from Proposition 6 (b) we get

$$P_L(\varepsilon Y; -\varepsilon) = \varepsilon P_L(Y; -1).$$

Thus, after such blow-up, Eq. (30) becomes

$$\varepsilon\,[F(Y; B) + \varepsilon G(Y, \varepsilon; B)] = 0, \qquad (31)$$

where

$$F(Y; B) = P_L(Y; -1) + Y - 2B$$

captures all the first order terms in ε of (31), and the analytical function $G(Y, \varepsilon; B)$ comes from the second and higher order terms in ε of P_R^{-1}, with

$$G(Y, 0; B) = \beta_2(Y - B)^2.$$

Note that for $\varepsilon \neq 0$ the bifurcation equation (31) leads to

$$F(Y; B) + \varepsilon G(Y, \varepsilon; B) = 0, \qquad (32)$$

so that if we know a zero $\overline{Y}$ of F then, under adequate hypotheses, we can apply the implicit function theorem to deduce the existence of a solution branch $Y(\varepsilon; B)$ of (32), and so of (31), with $Y(0; B) = \overline{Y}$.

To determine the zeros of F, we define for $Y \geq 0$ the function

$$H(Y) = P_L(Y; -1) + Y,$$

which from Proposition 5 (e) satisfies $H''(Y) < 0$ in its domain, and from Proposition 6 we know that

$$H(0) = -\alpha_0 < 0, \quad H'(0) = 1,$$

and

$$\lim_{Y\to\infty} H'(Y) = 1 - e^{\gamma_L \pi} < 0.$$

Therefore, the function H is unimodal, starting with a negative value, next increasing up to a maximum, and then decreasing to $-\infty$ when $Y \to \infty$. In fact, we can compute the maximum value of H as follows. We look for the unique value Y such that $H'(Y) = 0$, that is $P_L'(Y; -1) = -1$. From (17) we easily get the equivalent condition

$$P_L(Y; -1) = -Ye^{2\gamma_L t},$$

where t stands for the corresponding return time and then, from statement (b) of Proposition 6, we conclude that

$$\varphi_{\gamma_L}(t) = \varphi_{\gamma_L}(-t).$$

This last condition leads after standard manipulations to the equation

$$\tanh(\gamma_L t) = \gamma_L \tan t,$$

whose only solution in $(\pi, 2\pi)$ is a value $t_M < 3\pi/2$. Substituting this value in the parametric expressions of P_L, we get after simplifications

$$\max_{Y\geq 0} H(Y) = \frac{2\gamma_L}{\gamma_L^2 + 1}\left(\frac{\sinh(\gamma_L t_M)}{\gamma_L \sin(t_M)} - 1\right) < 0.$$

Since $F(Y; B) = H(Y) - 2B$,if we define

$$B_0 = -\frac{\alpha_0}{2}, \quad B_M = \frac{\gamma_L}{\gamma_L^2 + 1}\left(\frac{\sinh(\gamma_L t_M)}{\gamma_L \sin(t_M)} - 1\right),$$

then we can assure that for $B \in (B_0, B_M)$ the function F has exactly two zeros $0 < \overline{Y_1} < \overline{Y_2}$ with

$$0 < H'(\overline{Y_1}) < 1$$

and

$$1 - e^{\gamma_L \pi} < H'(\overline{Y_2}) < 0.$$

Note that

$$\frac{\partial F}{\partial Y}(\overline{Y_i}; B) = H'(\overline{Y_i}) \neq 0, \ i = 1, 2.$$

Thus, once selected B in such interval, we can apply the implicit function theorem to Eq. (32) at both values $\overline{Y_i}$ and $\varepsilon = 0$, to conclude the existence of two smooth

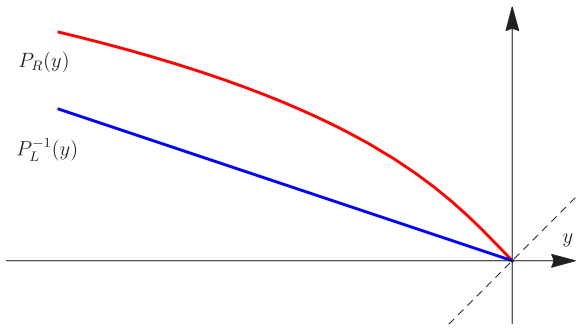

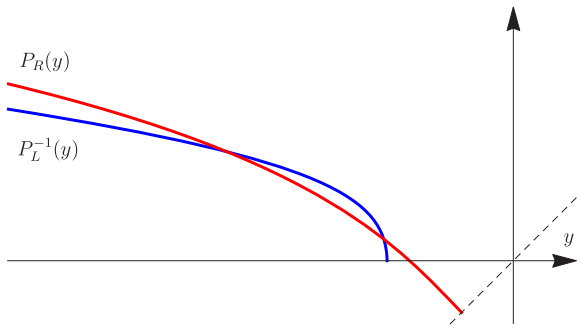

Fig. 4 Local sketch for graphs of the half-return maps $P_R(y)$ and $P_L^{-1}(y)$. The *dashed line* stands for the diagonal of the first quadrant. *Left panel* Under hypotheses of Proposition 3, both graphs start at the origin and have a intersection point far on the *left* (not shown). *Right panel* The perturbation considered in Proposition 4 of the above situation, adding two intersections points, to get three crossing periodic orbits in total. Note that the new graph of $P_R(y)$ is a mere translation of the original one, starting now at the point (b, b) with $b < 0$, while the graph of $P_L^{-1}(y)$ starts at the point $(P_L(0), 0)$

functions $Y_i(\varepsilon; B)$ with $Y_i(0; B) = \overline{Y_i}$, $i = 1, 2$, and defining solution branches of (31) and (32).

In short, by undoing the blow-up, we conclude that the number of positive solutions of (30) changes at two different values of b, namely at $b = \eta_i(a_L)$, $i = 1, 2$, where

$$\eta_1(a_L) = -B_0 a_L + O(a_L^2),\ \eta_2(a_L) = -B_M a_L + O(a_L^2).$$

Consequently, the Poincaré map P has two fixed points in the open parameter sector of the statement, which up to first order in $a_L = -\varepsilon < 0$ are $y_1 = -a_L\overline{Y_1}$ and $y_2 = -a_L\overline{Y_2}$.

Finally, an easy argument shows that if $Q'(y) > 0$ ($Q'(y) < 0$) at one solution of (30), then for the full Poincaré map we have $P'(y) < 1$ ($P'(y) > 1$), so that the periodic orbit is stable (unstable). Thus, the stability of the predicted periodic orbits comes from the sign of computed derivatives $H'(\overline{Y_i})$, $i = 1, 2$, and the proposition is proved. □

In Fig. 4, we use the graphs of half-return maps P_R and P_L^{-1} to visualize the effect of passing from the case $a_L = b = 0$ to the interior of the parameter sector analyzed in Proposition 4.

Acknowledgments Authors are partially supported by the Spanish Ministerio de Ciencia y Tecnologia, Plan Nacional I+D+I, in the frame of projects MTM2010-20907 and MTM2012-31821, and by the Consejería de Economía-Innovacíon-Ciencia-Empleo de la Junta de Andalucí a under grant P12-FQM-1658.

References

1. Andronov, A., Vitt, A., Khaikin, S.: Theory of Oscillations. Pergamon Press, Oxford (1966)
2. Artés, J.C., Llibre, J., Medrado, J.C., Teixeira, M.A.: Piecewise linear differential systems with two real saddles. Math. Comp. Sim. (2013). **95**, 13–22 (2013)
3. Braga, D.C., Mello, L.F.: Limit cycles in a family of discontinuous piecewise linear differential systems with two zones in the plane. Nonlinear Dynamics **73**, 1283–1288 (2013)
4. Braga, D.C., L.F, Mello: More than three limit cycles in discontinuous piecewise linear differential systems with two zones in the plane. Int. J. Bifurc. Chaos **24**, 1450056-1–1450056-10 (2014)
5. Buzzi, C., Pessoa, M., Torregrosa, J.: Piecewise linear perturbations of a linear center. Discrete Continuous Dyn. Syst. **9**, 3915–3936 (2013)
6. di Bernardo, M., Budd, C.J., Champneys, A.R., Kowalczyk, P.: Piecewise-Smooth Dynamical Systems: Theory and Applications. Appl. Math. Sci., vol 163. Springer-Verlag London Ltd., London (2008)
7. Freire, E., Ponce, E., Rodrigo, F., Torres, F.: Bifurcation sets of continuous piecewise linear systems with two zones. Int. J. Bifurc. Chaos **8**, 2073–2097 (1998)
8. Freire, E., Ponce, E., Torres, F.: Canonical discontinuous planar piecewise linear systems. SIAM J. Appl. Dyn. Syst. **11**, 181–211 (2012)
9. Freire, E., Ponce, E., Torres, F.: The discontinuous matching of two planar linear foci can have three nested crossing limit cycles. Publ. Mat. 221–253. doi:10.5565/PUBLMAT_Extra14_13 (2014)
10. Freire, E., Ponce, E., Torres, F.: On the critical crossing cycle bifurcation in planar filippov systems. (Preprint)
11. Guardia, M., Seara, T.M., Teixeira, M.A.: Generic bifurcations of low codimension of planar filippov systems. J. Differential Equations **250**, 1967–2023 (2011)
12. Han, M., Zhang, W.: On Hopf bifurcation in non-smooth planar systems. J. Differential Equations **248**, 2399–2416 (2010)

13. Huan, S., Yang, X.: On the number of limit cycles in general planar piecewise linear systems. Discrete Continuous Dyn. Syst. A **32**, 2147–2164 (2012)
14. Huan, S., Yang, X.: On the number of limit cycles in general planar piecewise linear systems of node-node types. J. Math. Anal. Appl. **411**, 340–353 (2013)
15. Huan, S., Yang, X.: Existence of limit cycles in general planar piecewise linear systems of saddle–saddle dynamics. Nonlinear Anal. **92**, 82–95 (2013)
16. Llibre, J., Teixeira, M.A., Torregrosa, J.: Lower bounds for the maximum number of limit cycles of discontinuous piecewise linear differential systems with a straight line of separation. Int. J. Bifurc. Chaos. 23, (2013). doi:10.1142/S0218127413500661
17. Llibre, J., Ponce, E.: Three nested limit cycles in discontinuous piecewise linear differential systems. Dyn. Continuous Discrete Impuls. Syst. B **19**, 325–335 (2012)
18. Shui, S., Zhang, X., Li, J.: The qualitative analysis of a class of planar Filippov systems. Nonlinear Anal. **73**, 1277–1288 (2010)
19. Simpson, D.J.W.: Bifurcations in Piecewise-Smooth Continuous Systems. World Scientific Series on Nonlinear Science A, vol 69. World Scientific, Singapore (2010)